Joint Position and Orientation Estimation in VCSEL-Based LiFi Networks: A Deep Learning Approach

Rizwana Ahmad, Hossein Kazemi, Elham Sarbazi, Harald Haas
LiFi Research and Development Center, University of Strathclyde, Glasgow, UK.
Email: {rizwana.ahmad, h.kazemi, e.sarbazi, harald.haas}@strath.ac.uk

***Abstract*—To enable intelligent network management and various 6G smart services, the precise estimation of user location and device orientation is required. Light fidelity (LiFi) based on vertical cavity surface emitting lasers (VCSELs) can not only respond to the needs of 6G communication networks in terms of ultra-high data rate, connection density and area capacity, but also enable high precision position and orientation estimation. However, this problem of joint position and orientation estimation is a non-convex optimization problem. Therefore, in this paper, we design deep neural networks (DNNs) for joint position and orientation estimation of user devices in a VCSEL-based LiFi access network. Simulation results demonstrate that the proposed framework outperforms state-of-the-art methods by significantly reducing position and orientation estimation errors while maintaining a lower complexity. We illustrate the effectiveness of the proposed DNN solution by considering two types of network deployment including distributed VCSELs and collocated VCSELs. In addition, we present the convergence and complexity analysis for the proposed learning framework. It is shown that the proposed DNN provides at least 69% and 27.9% improvements in the mean estimation error for position and orientation, respectively, over the baseline method.**

***Index Terms*—LiFi, 6G, indoor localization, orientation estimation, vertical cavity surface emitting laser (VCSEL).**

I. Introduction

Sixth generation (6G) networks are envisioned to meet the demands of green communication, massive device connectivity, seamless coverage, full intelligence, and autonomous systems required for the 2030 intelligent information society. Diverging from current communication networks, 6G networks will not be limited to moving data, rather it will intelligently process data in real time to provide various smart services. While achieving ultra-high aggregate data rates of Tbps, increased area traffic capacity of 1 Gbps/m^2, and improved security and privacy are key performance objectives of 6G, joint communication and sensing is an indispensable requirement for efficient operation of next generation networks [1]. In particular, high precision positioning information is required for smart services such as augmented reality, context-aware marketing, asset tracking, and autonomous systems. Therefore, next-generation networks require a technology that can simultaneously enable high-speed communication and precise localization.

Light fidelity (LiFi) is one such promising technology that can enable ultra-high data rates, improved connection density, and precise positioning. Although LiFi has a wide unlicensed spectrum, the achievable data rate of a LiFi communication link is usually limited by either the transmitter or receiver. The LiFi transmitter bottleneck is often due to characteristics of light-emitting diodes (LEDs) as they suffer from poor electrical-to-optical conversion efficiency and limited bandwidth. Nonetheless, it is possible to overcome this bottleneck by using laser diode (LD)-based LiFi transmitters as they have a better conversion efficiency, a higher modulation bandwidth, and well-controlled light beam properties. The LiFi receiver bottleneck, on the other hand, arises from the area-bandwidth and gain-field of view (FOV) trade-offs of photodiodes (PDs). In general, a smaller PD has a larger bandwidth and a higher optical gain is achieved for a lower FOV. Thus, an LD-based LiFi transmitter in conjunction with a smaller, low FOV receiver is preferred for 6G applications as it can support ultra-high data rate requirements.

Concerning the precise knowledge of the receiver location and orientation, achieving sub-cm level localization accuracy in an indoor environment is a major challenge. The widely accepted global positioning system (GPS)-based localization is neither applicable, nor accurate enough for indoor scenarios due to high signal attenuation caused by building infrastructure. Thus, non-GPS localization solutions are desirable for indoor environments. Although WiFi and Bluetooth can be used for indoor positioning, they have positioning errors ranging between 1–7 m and 2–5 m, respectively [2]. In contrast, LiFi-based indoor positioning systems can achieve better localization performance with a positioning error of 0.1–0.35 m. As LiFi uses directional light beams for communication, it is also crucial to estimate the orientation of connected devices for optimal performance of the system. However, joint position and orientation estimation for LiFi users is challenging due to the complex and nonlinear interplay between received signal-to-noise ratio (SNR), user orientation, and location. Traditional methods like the maximum likelihood estimator result in multiple local minima and require additional information such as initial position, prior estimation of orientation, or additional infrastructure and an iterative algorithm [2], [3]. However, intelligent deep learning (DL) methods can efficiently solve this non-convex optimization problem of joint orientation and position estimation at a relatively lower complexity without the need for additional information and iterative algorithm.

Table I summarizes the existing DL-enabled LiFi indoor positioning solutions [2], [4]–[7]. Only the work in [2] considers DL based joint position and orientation estimation based on the practically feasible approach of received SNR. Thus,

TABLE I: Related work on machine learning (ML)-based position and orientation estimation for LiFi

Reference	Method	LD	Position estimation	Orientation estimation	Positioning error[1] [cm]	Complexity	Remark
[2]	SNR based deep neural network (DNN), convolutional neural network (CNN) and k-nearest neighbors (KNN).	✗	✓	✓	Mean, $= 10.5$ Precision[2], $= 17.2$	An estimation time of 0.20 ms	FOV $= 90°$.
[4]	RSS based Weighted K-Nearest Neighbor (WKNN).	✗	✓	✗	Mean $= 7$ Precision[1] $= 21$	Not included.	Accuracy degraded with reduction in light-sensors.
[5]	Channel impulse response (CIR) based DNN, CNN and long short-term memory (LSTM) solution.	✗	✓	✗	Mean $= 4.2$ Precision[2] $= 5.6$	Estimation time ranges from 23 to 64 ns.	FOV $= 85°$ CIR collection is computationally intensive.
[6]	Uses CIR of 9 LED-PD pairs and fully connected NN.	✗	✓	✗	For high SNR Root-mean-square error (RMSE) $= 30$	Complexity reduces with increasing bin sizes.	CIR collection is computationally intensive.
[7]	Multi-task Federate learning for spatial generalization using cluster approach.	✗	✓	✗	For SNR $= 35$ dB: Mean $= 6.7$ Precision[2] $= 10$	Not included.	FOV $= 90°$.
This Work	VSCELs received SNR is exploited for joint position and orientation estimation using DNN.	✓	✓	✓	**Mean $= 4.5$** **Precision[2] $= 8.72$**	Quantitative analysis included.	FOV $= 60°$ (More practical).

[1]Best possible position error reported in the reference.
[2]Represents the 90^{th} percentile obtained using CDF of the position error (i.e., 90% of the estimation errors are below the precision value).

in this work, we consider [2] as the baseline reference for comparison. All these works [2], [4]–[7] employed LED-based LiFi systems with a low bandwidth (i.e., ≤ 100 MHz) and a very high receiver FOV (i.e., $85°$–$90°$). These specifications are not suitable for multi-Gbps transmission rates required in 6G networks. By contrast, a laser-based LiFi system can significantly improve both the localization and data rate performance. In [8], the authors have shown that an array of arrays of vertical cavity surface emitting lasers (VCSELs) can safely achieve beyond Tbps aggregate capacities. In particular, VCSELs have a bandwidth > 1 GHz, a low manufacturing cost, and a narrow spectral width. The high-quality output beam of VCSELs can be leveraged for precise indoor positioning as well.

In this paper, we propose a deep neural network (DNN) structure for joint position and orientation estimation of users in a VCSEL-based LiFi networks. The recommended DNN approach does not require specific number of active links, nor does it need prior knowledge about the position and orientation of the user device. While it is possible to implement a more sophisticated neural network (NN) such as a convolutional neural network (CNN), for our study, we utilized the simplest NN in order to ensure good performance without introducing too much computation overload on the system. We illustrate the effectiveness of the proposed DNN solution for two different VCSEL deployments, namely distributed VCSELs and collocated VCSELs. We consider a more realistic framework in this work with random user device orientation, blockages, and a smaller receiver FOV. In addition, we develop the algorithm for dataset generation which can be used as a reference for future works. We also present the convergence analysis of the proposed DNN. Through a comparison with the baseline method by Arfaoui *et al.* [2], we show that the proposed DNN achieves a superior performance in terms of the mean and precision of position and orientation errors as well as the computational complexity.

The rest of the paper is organized as follows. The system model is described in Section II. The learning framework for joint position and orientation estimation along with details related to dataset generation and training convergence are introduced in Section III. Performance evaluation and discussions are presented in Section IV, and conclusions are given in Section V.

II. System Model

We consider localization of a LiFi user based on DNN in a room of size $1 \times 1 \times 3$ m^3 by using a 5×5 array of VCSELs. Fig. 1 shows two possible configurations for the VCSEL array: a) distributed VCSELs and b) collocated VCSELs. In the distributed configuration, the VCSELs are evenly distributed on the ceiling to provide uniform coverage for the network. In the collocated configuration, on the contrary, the VCSELs are located close to one another at the center of the ceiling. While the distributed VCSELs configuration uses a simpler transmitter design (i.e., a single VCSEL with or without optics), it needs high-capacity back-haul connections between individual access points (APs) which introduces more complexity and delay, thus, limits the overall system performance. In contrast, the collocated VCSELs configuration is easier to manage and deploy, but its single transmitter requires an appropriate optical design (e.g., plano-convex lens) in order to obtain a spatially separated intensity profile for multiple laser beams. The optical front-end design for such an AP is beyond the scope of this paper; see [8] for more details.

A. Channel Modeling

The output profile of a single-mode VCSEL can be modeled by a Gaussian beam, as shown in Fig. 2. The intensity distribution for a Gaussian beam is expressed as follows [8]:

$$I(r_0, d_0) = \frac{2P_{\text{opt}}}{\pi w^2(d_0)} \exp\left(-\frac{2r_0^2}{w^2(d_0)}\right), \tag{1}$$

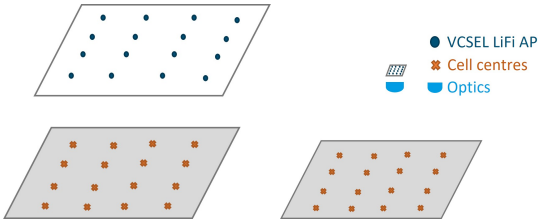

(a) Distributed VCSELs (b) Collocated VCSELs

Fig. 1: Two configurations for VCSEL array deployment.

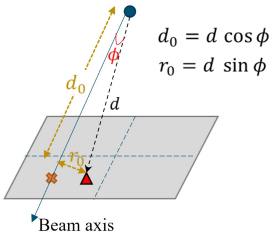

Fig. 2: Channel model based on Gaussian beam propagation.

TABLE II: Truncated Laplace distribution parameters for the three rotation angles of the LiFi receiver.

	α	β	γ
Mean	$\Omega - 90°$	$28.81°$	$-1.35°$
Standard deviation	$10°$	$3.26°$	$5.42°$

where P_{opt} is the optical power carried by a single VCSEL beam; r_0 and d_0 represent the radial distance and the axial position, respectively, on the receiver plane in the cylindrical coordinate system. The beam spot radius is given by:

$$w(d_0) = w_0\sqrt{1+\left(\frac{\lambda d_0}{\pi w_0}\right)^2}, \quad w_0 = \frac{\lambda}{\pi\theta_{\text{beam}}} \tag{2}$$

where w_0 is beam waist radius, with λ and θ_{beam} denoting the operating wavelength and the far-field divergence angle of the beam. Let, ϕ denote the radiance angle at the VCSEL transmitter with respect to the receiver direction. Then, the beam intensity in (1) can be written as:

$$I(d,\phi) = \frac{2P_{\text{opt}}}{\pi w^2(d\cos\phi)}\exp\left(-\frac{2d^2\sin^2\phi}{w^2(d\cos\phi)}\right). \tag{3}$$

Thus, the received optical power can be obtained using [9]:

$$P_{\text{r}} = I(d,\phi)A_{\text{PD}}\cos\psi\,\text{rect}\left(\frac{\psi}{\Psi}\right), \tag{4}$$

where A_{PD} is the effective PD area, ψ is the incidence angle at the receiver, and $\text{rect}(\psi/\Psi) = 1$ for $0 \le \psi \le \Psi$, and 0 otherwise, with Ψ denoting the half-angle FOV of the receiver. The corresponding received SNR is given by:

$$\text{SNR} = \frac{(R_{\text{PD}}P_{\text{r}})^2}{\sigma_{\text{n}}^2}, \tag{5}$$

with R_{PD} is the PD responsivity, and σ_{n}^2 is the noise variance.

B. User Orientation Modeling

Since alignment between the transmitter and receiver plays a major role in the performance of laser-based LiFi systems, it is imperative to accurately model the receiver orientation. In general, the orientation of a LiFi user can be modeled by using three angles of yaw α, pitch β, and roll γ, for rotations about the z, x and y axes, respectively. In [10], through experimental measurements, it is shown that these three angles follow a truncated Laplace distribution with their respective mean and standard deviation values, as listed in Table II. The mean of α depends upon the Ω which is defined according to the direction of movement [10].

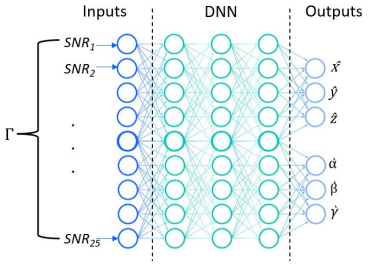

Fig. 3: Proposed DNN model for joint estimation of the LiFi receiver position and orientation.

C. Eye Safety

One of the crucial practical challenges of utilizing laser beams for indoor LiFi communications is to ensure the eye safety of users. According to laser safety regulations defined by the international electrotechnical commission (IEC) 60825 standard [11], the eye safety assessment involves determining the optical power level at the most hazardous position (MHP). For single-mode Gaussian beams, the maximum permissible optical power primarily depends on the laser wavelength λ and the beam waist radius w_0. Based on [12], for a Gaussian laser beam with $w_0 = 5$ µm, the maximum permissible optical power can be calculated as $P_{\text{opt,max}} = 16$ mW. In this work, we consider $P_{\text{opt}} = 10$ mW for each VCSEL to fulfill the eye safety constraint.

III. Joint Position and Orientation Estimation Using Deep Neural Network

In this section, we put forward the design of a DNN to jointly estimate the LiFi user position $(\hat{x},\hat{y},\hat{z})$ and orientation $(\hat{\alpha},\hat{\beta},\hat{\gamma})$ by exploiting the received SNR from multiple beams. The proposed DNN, as shown in Fig. 3, is made up of multiple layers which can mainly be classified into three categories: a) input, b) hidden, and c) output layer. The received SNR from N_{VCSELs} are fed into the input layer and they are processed by three hidden layers, each of which is composed of 100, 50, and 20 neurons, respectively. Each hidden layer is followed by a dropout layer which randomly removes individual neurons with a certain probability during the training phase to avoid overfitting. The activation function used at each hidden layer is a rectified linear unit (ReLU) activation function. The output layer comprises six neurons ($N_{\text{out}} = 6$), each of which is responsible for estimating one of the six parameters $(\hat{x},\hat{y},\hat{z},\hat{\alpha},\hat{\beta},\hat{\gamma})$. The DNN needs to be trained to learn the unique mapping between the received SNR and the receiver position and orientation.

Algorithm 1 Algorithm for dataset generation.

Input: Total number of data points $\mathcal{N}$, number of VCSELs N_{VCSEL}, statistical distribution for orientation angles, and blockage probability P_{b}.
Output: Γ: dataset with $\mathcal{N}$ received SNR data points.

while $i \in \mathcal{N}$ **do**
  Use the following uniform distributions to obtain the 3D position of the user device, (x_i, y_i, z_i):

$$\begin{aligned} f_x(x) &= \mathcal{U}[0, L] \\ f_y(y) &= \mathcal{U}[0, W] \\ f_z(z) &= \mathcal{U}[H_{\min}, H_{\max}] \end{aligned} \tag{6}$$

  Use the statistical parameters defined in Table II to obtain the three rotation angles α_i, β_i , and γ_i.
  Use the above rotation angles to determine the normal vector of the user device at the i^{th} location based on [10]:

$$n_i = \begin{bmatrix} \cos\gamma_i \sin\alpha_i \sin\beta_i + \cos\alpha_i \sin\gamma_i \\ \sin\alpha_i \sin\gamma_i - \cos\alpha_i \cos\gamma_i \sin\beta_i \\ \cos\gamma_i \cos\beta_i \end{bmatrix} \tag{7}$$

  while $j \in N_{\mathrm{VCSEL}}$ **do**
    Obtain the distance $d_{j,i}$ and radiance angle $\phi_{j,i}$ between the j^{th} VCSEL and the i^{th} location (x_i, y_i, z_i).
    Use the normal vector n_i to determine the angle of incidence ψ at the receiver.
    Compute $\mathrm{SNR}_{j,i}$ based on (5).
  end while
  Store SNR_i in Γ.
end while
if Blockage **then**
  Find the probability of blockage using the Poisson distribution [13]:

$$P_{\mathrm{b}} = \frac{\lambda_{\mathrm{b}}^k e^{-\lambda_{\mathrm{b}}}}{k!} \tag{8}$$

  where λ_{b} is the expected occurrence rate which defines the average number of blockages that occur in a time unit, and k denotes the number of blockages.
  To include the effect of blockages in the system, set $P_{\mathrm{b}} \times \mathcal{N}$ random values in Γ to 0.
end if

A. Dataset Generation

Since no preexisting dataset is available for joint position and orientation estimation in VCSEL-based LiFi networks, we have developed a MATLAB program for this purpose. The steps involved in the dataset generation procedure are summarized in Algorithm 1. This algorithm provides dataset Γ with $\mathcal{N}$ received SNR data points. In our work, the dataset comprises a total of 10^5 data points and it is divided into a 70/30 ratio to obtain training and validation dataset.

B. DNN Training and Convergence

The DNN training consists of selecting the best set of neural network parameters (i.e., weights and biases) that minimize the error metric between the actual values of $(x, y, z, \alpha, \beta, \gamma)$ and their estimated values $(\hat{x}, \hat{y}, \hat{z},\ \hat{\alpha}, \hat{\beta}, \hat{\gamma})$. The proposed DNN structure, shown in Fig. 3, has 8775 trainable parameters in total. During the training phase, the values for these parameters are learned based on the Adam optimizer (with learning rate=0.001) by minimizing the mean absolute error between the actual and estimated values. The corresponding training loss and validation loss for the two VCSEL array configurations are shown in Fig. 4. The training and validation loss are the mean absolute loss values calculated over the training and validation set. They illustrate how well the model fits the data. It can be observed that for both configurations, the training and validation loss converges to a certain value even in the presence of blockages. Note that the absolute value of loss is slightly higher when a number of beams are randomly blocked with an average blockage rate of $\lambda_{\mathrm{b}} = 10\%$, which happens due to the missing data points as a result of the blocked links. This highlights the fact that the occurrence of blockages adversely affects the localization accuracy. Furthermore, from Fig. 4, it can be observed that both the training and validation losses decrease with increasing epoch indexes and stabilizes after some epochs. This trend of validation loss confirms that the designed DNN is not over-fitting and it can be generalized well for unseen data points even in the case of blockages.

IV. Performance Evaluation and Discussion

In this section, the performance of the proposed DNN (Section III) is evaluated under the two deployment configurations for the VCSEL-based indoor LiFi network, as shown in Fig. 1. In order to create the dataset and build the proposed neural network, we have implemented Algorithm 1 using MATLAB 2021 and designed the DNN using Python 3.7. Table III lists the system parameters used for simulations. The system performance is evaluated in terms of the following metrics:

- Mean error μ: the average of the estimation errors.
- Precision error δ: the 90^{th} percentile of the estimation errors, so that 90% of the estimation errors are below δ.
- Complexity: the run-time complexity expressed in terms of big-$\mathcal{O}$ notation.

A. Effectiveness of the Proposed DNN

The effectiveness of the proposed DNN is examined for different deployments and under blockage conditions as follows:

1) Different Deployments: Fig 5 illustrates the cumulative distribution function (CDF) of the instantaneous position and orientation estimation errors for both configurations. While the orientation error is almost similar for the two configurations, the position error is slightly higher in the case of collocated VCSELs. More specifically, the difference in the CDFs of the position error is more prominent for x and y coordinates as compared to the z coordinate. Nonetheless, there is a marginal difference between the CDFs for the two configurations, which corroborates the effectiveness of the proposed DNN.

2) Performance in the Presence of Blockages: Figs. 6 and 7 illustrate the mean error and the precision error of the proposed solution versus the average blockage rate λ_{b} in the presence of blockages for distributed and collocated VCSEL deployments, respectively. The case of $\lambda_{\mathrm{b}} = 0$ indicates the blockage-free system. It can be observed that as the average blockage rate increases, both the mean and precision errors also increase. This is expected because with a higher average blockage rate, the DNN receives a proportionally lesser number of SNRs, which in turn reduces the estimation accuracy.

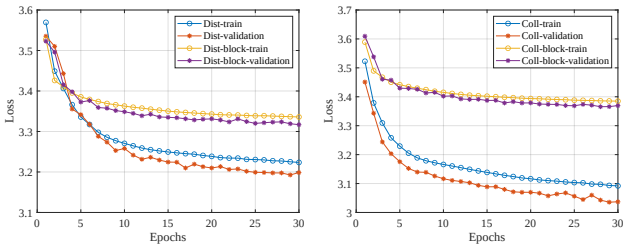

(a) Distributed VCSELs (b) Collocated VCSELs

Fig. 4: Training and convergence of the proposed DNN.

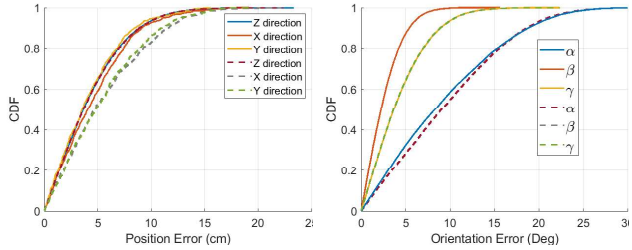

Fig. 5: CDF of error for different VCSEL deployments: distributed VCSELs (solid line) and collocated VCSELs (dashed line).

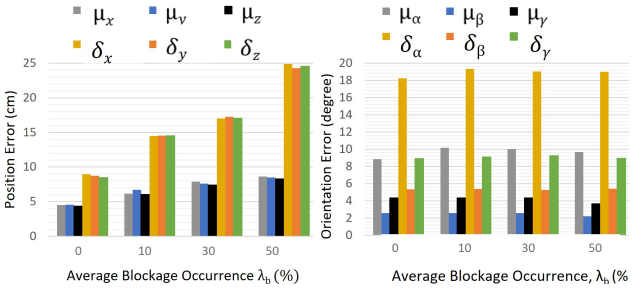

Fig. 6: Mean error μ and precision error δ for distributed VCSELs for different values of the average blockage occurrence rate $\lambda_{\rm b}$.

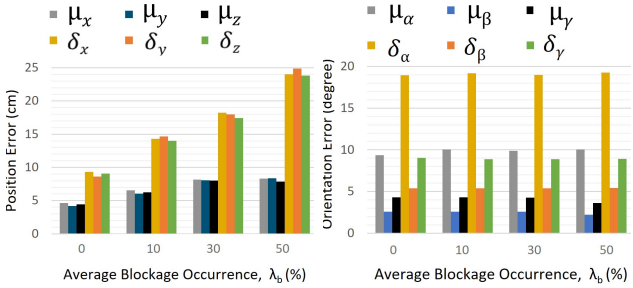

Fig. 7: Mean error μ and precision error δ for collocated VCSELs for different values of the average blockage occurrence rate $\lambda_{\rm b}$.

Note that the introduction of blockages into the system has a greater impact on the position estimation than the orientation estimation. This is due to the inherent difference in the statistical distributions considered for orientation angles (truncated Laplace) and position (Uniform). However, the mean value for α varies with Ω, and as a result it is hard for the DNN to learn the exact mapping between the SNR values and α. For this reason, the estimation of α leads to the worst mean and precision errors.

Overall, the proposed DNN works well for small values of the average blockage rate for $\lambda_{\rm b} = 10, 30\%$. This is primarily due to the fact that the DNN uses data from multiple VCSELs, with $N_{\rm VCSEL} = 25$. Thus, in random realizations for smaller values of $\lambda_{\rm b}$, the expected number of times that the most useful SNR undergoes a blockage is lower. However, for larger values of $\lambda_{\rm b}$, the DNN may not receive any of the useful SNRs to correctly estimate the position and orientation.

B. Comparison with Baseline

1) Estimation Error Performance: The performance of the proposed method is compared against the baseline system [2]. For a fair comparison, we only consider the position error and the yaw angle error α, as the authors in [2] converted the other two angles, β and γ, into a single angle in their final results. In addition, the same dataset size of $\mathcal{N} = 10^5$ is assumed for both the proposed and baseline systems. Furthermore, no blockage ($\lambda_{\rm b} = 0\%$) is considered in the system for fair comparison. However, the best performance of the baseline system was achieved by using a CNN. Hence, the performance of the proposed method is compared against both cases of the baseline CNN and DNN methods [2].

Table IV compares the estimation error performance of the proposed DNN method with those achieved by the baseline methods. It can be observed that the proposed method significantly reduces the mean position estimation error by around 10 cm which translates to an improvement in the mean position estimation by 69% and 70% over the baseline CNN and DNN methods, respectively. Similar performance improvements are observed for the precision value of the position error. The proposed method reduces the position error precision to a significantly smaller value of 8.72 cm as compared to 23.9 cm and 25 cm in the baseline-CNN and baseline-DNN cases, respectively.

The proposed DNN also outperforms both the baseline methods in terms of the mean and precision of the orientation estimation error for α, with the corresponding improvements of 27.9% and 29.5% over the baseline-CNN and baseline-DNN. It can be observed that the proposed DNN provides at least 69% and 27.9% improvements in the mean position and orientation estimation errors over the baseline.

2) Complexity: The run-time complexity of the proposed learning framework is compared against the baseline [2] in terms of big-$\mathcal{O}$ notation. We assume that the DNN has an $N_{\rm in}$-dimensional input, an $N_{\rm out}$-dimensional output and K hidden layers each with M_k neurons where $k \in \{1, 2, ...K\}$. In this case, the number of multiplications required is $\mathcal{O}(N_{\rm in}M_1 + M_1M_2 + ... + M_{k-1}M_k + M_kN_{\rm out})$. Based on the proposed DNN, its complexity is given by $\mathcal{O}(N_{\rm VCSELs} \times 100 + 100 \times 50 + 50 \times 20 + 20 \times N_{\rm out})$. Also, using the specification of baseline-DNN given in [2], the complexity of the baseline-DNN is given by $\mathcal{O}(N_{\rm LED} \times 256 + 256 \times 256 + 256 \times 256 + 256 \times N_{\rm out})$. Similarly, we assume that the CNN has an $N_{\rm in}$-dimensional input and an $N_{\rm out}$-dimensional output, a filter or kernel size of F, and K hidden layers each with M_k neurons. The corresponding run-time complexity is given by $\mathcal{O}(N_{\rm in}FM_1 + M_1FM_2 + ... + M_{k-1}FM_k + M_kFN_{\rm out})$. For the baseline-CNN, using the specification given in [2], the resulting

TABLE III: System parameters.

Parameter	**Value**
Length L × Width W × Height H	$1 \times 1 \times 3$ m^3
User height range, $[H_{\min}, H_{\max}]$	$[0.5, 1.5]$ m
Number of VCSELs, N_{VCSEL}	25 (5×5 array)
VCSEL wavelength, λ	950 nm
Beam waist radius, w_0	5.9 μm
Transmit power per VCSEL, P_{opt}	10 mW
System bandwidth, B	1 GHz
PD FOV, Ψ	60°
Effective PD area, A_{PD}	1 cm^2
Load resistance, R_{L}	50 Ω
PD responsivity, R_{PD}	0.5 A/W
Average blockage occurrence rate, λ_{b}	$0, 10\%, 30\%, 50\%$

TABLE IV: Performance comparison with baseline.

Estimation error		Proposed DNN	Baseline	
			CNN	DNN
Position	mean, μ	4.51 cm	14.55 cm	15.05 cm
	precision, δ	8.72 cm	23.9 cm	25.1 cm
Orientation (α)	mean, μ	8.85°	12.28°	12.56°
	precision, δ	18.23°	18.5°	18.9°

TABLE V: Complexity comparison with baseline.

	Run-time complexity
Proposed DNN	$\mathcal{O}(N_{\text{VCSEL}} \times 100 + 20 \times N_{\text{out}})$
Baseline-CNN [2]	$\mathcal{O}(N_{\text{LED}} \times 16 \times 64 + 64 \times 16 \times N_{\text{out}})$
Baseline-DNN [2]	$\mathcal{O}(N_{\text{LED}} \times 256 + 256 \times N_{\text{out}})$

run-time complexity becomes $\mathcal{O}(N_{\text{LED}} \times 16 \times 64 + 64 \times 16 \times 64 + 64 \times 16 \times 64 + 64 \times 16 \times N_{\text{out}})$. Table V summarizes the run-time complexities for different methods in a simplified form. It is evident that the proposed DNN has a lower complexity than the baseline.

V. Conclusion

In this paper, for the first time, the idea of using an array of VCSELs was introduced to achieve sub-centimeter positioning accuracy in a high-speed LiFi network. Specifically, a DNN was designed for joint position and orientation estimation for a LiFi receiver with random location and rotation angles. The effectiveness of the proposed DNN was verified for different VCSEL deployment configurations and in the presence of low average blockages. The proposed DNN was able to achieve high-precision positioning and orientation angle estimation for all the considered scenarios without any prior knowledge or assumptions about the LiFi network.

The performance of the proposed DNN was compared with state-of-the-art results in [2], in terms of the mean estimation error, the precision error, and the computational complexity. It was shown that the proposed DNN outperforms the baseline methods by providing an improvement of at least 69% and 27.9% in the mean position and orientation estimation errors over the baseline [2]. In addition, the proposed DNN has a significantly lower complexity which means that the proposed network trains and estimates faster than the baseline methods.

In this study, the proposed DNN was effective for smaller average blockages rates of $\lambda_{\text{b}} = 10, 30\%$, however, for larger blockage rates its performance was compromised as the most useful links were blocked. For larger blockage probabilities, an angle diversity receiver (ADR) can help in collecting useful signals to effectively estimate the position and orientation of the receiver even under very high blockages. This constitutes an interesting direction for future research. Additionally, the current work considers the simplest DNN structure for proof of concept, considering more advanced DL methods can help further improve the performance at the cost of increased complexity. Thus, another future direction of this work can be towards exploring multi-task learning for integrated communication and sensing.

Acknowledgment

This work is a contribution by Project REASON, a UK Government funded project under the Future Open Networks Research Challenge (FONRC) sponsored by the Department of Science Innovation and Technology (DSIT).

References

[1] Qadir, Zakria, et al., "Towards 6G internet of things: Recent advances, use cases, and open challenges," *ICT Express*, 2022.

[2] M. A. Arfaoui, M. D. Soltani, I. Tavakkolnia, A. Ghrayeb, C. M. Assi, M. Safari, and H. Haas, "Invoking deep learning for joint estimation of indoor LiFi user position and orientation," *IEEE Journal on Selected Areas in Communications*, vol. 39, no. 9, pp. 2890–2905, 2021.

[3] S. Shen, S. Li, and H. Steendam, "Hybrid position and orientation estimation for visible light systems in the presence of prior information on the orientation," *IEEE Transactions on Wireless Communications*, vol. 21, no. 8, pp. 6271–6284, 2022.

[4] N. Faulkner, F. Alam, M. Legg, and S. Demidenko, "Watchers on the wall: Passive visible light-based positioning and tracking with embedded light-sensors on the wall," *IEEE Transactions on Instrumentation and Measurement*, vol. 69, no. 5, pp. 2522–2532, 2019.

[5] X. Lin and L. Zhang, "Intelligent and practical deep learning aided positioning design for visible light communication receivers," *IEEE Communications Letters*, vol. 24, no. 3, pp. 577–580, 2019.

[6] K. Majeed and S. Hranilovic, "Passive indoor visible light positioning system using deep learning," *IEEE Internet of Things Journal*, vol. 8, no. 19, pp. 14 810–14 821, 2021.

[7] T. Wei, S. Liu, and X. Du, "Visible light integrated positioning and communication: A multi-task federated learning framework," *IEEE Transactions on Mobile Computing*, pp. 1–18, 2022.

[8] E. Sarbazi, H. Kazemi, M. Dehghani Soltani, M. Safari, and H. Haas, "A Tb/s indoor optical wireless access system using VCSEL arrays," in *2020 IEEE 31st Annual International Symposium on Personal, Indoor and Mobile Radio Communications*, 2020, pp. 1–6.

[9] Z. Zeng, M. D. Soltani, M. Safari, and H. Haas, "A VCSEL array transmission system with novel beam activation mechanisms," *IEEE Transactions on Communications*, vol. 70, no. 3, pp. 1886–1900, 2021.

[10] M. D. Soltani, A. A. Purwita, Z. Zeng, H. Haas, and M. Safari, "Modeling the random orientation of mobile devices: Measurement, analysis and LiFi use case," *IEEE Transactions on Communications*, vol. 67, no. 3, 2019.

[11] *Safety of Laser Products - Part 5: Manufacturer's Checklist for IEC 60825-1*, International Electrotechnical Commission (IEC) Std., 2019.

[12] R. Henderson and K. Schulmeister, *Laser safety*. CRC Press, 2003.

[13] X. Wu and H. Haas, "Load balancing for hybrid LiFi and WiFi networks: To tackle user mobility and light-path blockage," *IEEE Transactions on Communications*, vol. 68, no. 3, pp. 1675–1683, 2019.